

THE ROLE OF SiO₂ GAS IN THE OPERATION OF ANTI-CORROSION COATING PRODUCED BY PVD

Meysam Zarchi*, Shahrokh Ahangarani

Advanced Materials & Renewable Energies Department, Iranian Research Organization for Science and Technology, Tehran, Iran

Received 24.10.2014

Accepted 28.08.2015

Abstract

This study examined the SiO₂ gas present in the coatings used in corrosion industry. These layers have been created by physical vapor deposition (PVD), with an appropriate performance. Sublimation of SiO₂ is used to protect PVD aluminum flakes from water corrosion and to generate highly porous SiO₂ flakes with holes in the nanometer range. SiO_x/Al/SiO_x sandwiches were made as well as Ag loaded porous SiO₂ as antimicrobial filler.

Key words: PVD, Porous, Coat, SiO_x, Corrosion

Introduction

Popular liquid metal colors require the use of mirror-like aluminum pigment manufactured in a high vacuum process, i.e. physical vapor deposition (PVD). This equipment consists of an arc with a diameter of just a few microns running over the solid, metallic coating material, causing it to evaporate. Because of the high currents and power densities used, the evaporated material is almost totally ionized and forms high-energy plasma. Figure 1 shows a schematic a system of PVD. It was used to form of sandwich layers.

One application of this method is to achieve anti-corrosion coatings. Purely inorganic, transparent coatings have been developed for the corrosion protection of aluminum alloys, based on commercially available, aqueous SiO_x nano dispersions coatings.

These coatings can be processed under mild conditions, but are permeable for aggressive anions. The permeability can be decreased by sealing with inorganic polymeric sols. Despite their low thickness the resulting coatings show remarkable protective properties. Other features of these coatings, optical reflectance properties of

* Corresponding author: MeysamZarchi, sky_man1983@yahoo.com

them. Best optical reflectivity was achieved with flake thicknesses around 40 nanometers [1]. The reaction in water of neat Al flakes is a well know issue and various surface treatments have been proposed [2, 3]. SiO_2 as gas barrier against Al corrosion has been discussed in [4] and is known for a long time [5].

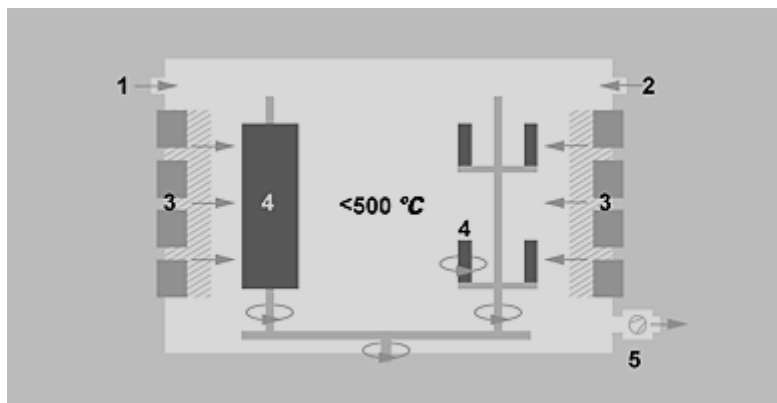


Figure 1. The schematic device used in the manufacture of sandwich layers; 1. Argon; 2. Reactive gas; 3. Arc sources (coating material and backing plate); 4. Components; 5. Vacuum pump

A high vacuum process to sandwich PVD Al between two SiO_x layers made by SiO_2 sublimation has been investigated in an attempt to protect PVD Al in water environment. A similar high vacuum process lead to highly porous SiO_x flakes.

Experimental

A high vacuum chamber is equipped with 4 evaporation sources (Joule heating) and 4 thickness measurement units. Al is evaporated by the conventional flash method. SiO_x preparation and sublimation are described elsewhere [6].

A water soluble release layer is first evaporated on a continuous carrier; Al and SiO_x are then evaporated, respectively sublimed, in desired order on the release layer. The carrier is removed from the vacuum chamber, the water soluble release layer is dissolved and the inorganic flakes are collected. A well-known release layer is NaCl [7]. Water soluble organic release layers can also be employed, among them pentaerythritol [8]. Vapor pressure of SiO_x [9] and NaCl [10] are high enough to allow high evaporation rates at moderate temperatures.

The optical reflectivity of the single SiO_x thin films deposited on the wafers was determined using a Hitachi U-5241 scanning micro photo spectrometer in the wavelength region 530-2200 nm. The spot size was 5 microns.

Results

SiO_x protected Al flakes

The sandwich structure of a particle of $\text{SiO}_x/\text{Al}/\text{SiO}_x$ ($x \sim 1.8$ to 2) is shown in Figure 2. The aluminum layer of 30 to 50 nm is situated between two homogenous SiO_x layers of 10 to 20 nm each. The SiO_x layers are acting as gas barriers to protect the Al

from further degradation by water for example. The particle side is bare, unprotected Al, but represents a small portion of the whole surface. No further surface modification was made on the present sample. The effect of the difference in thermal expansion between SiO_x and Al has not been investigated.

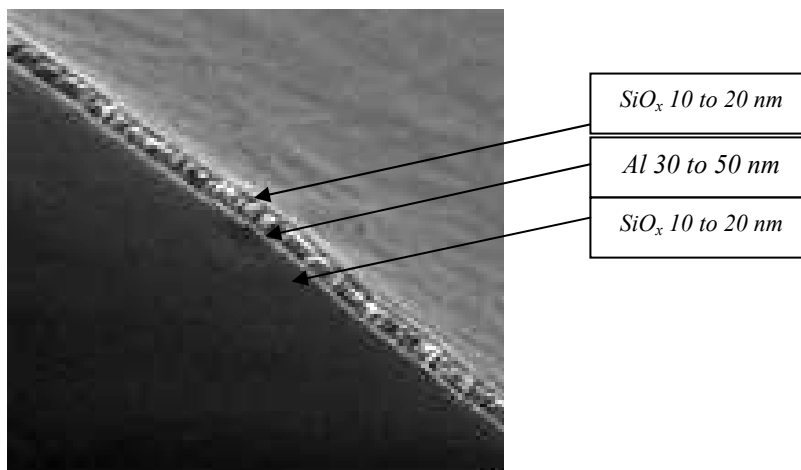


Figure 2. SEM micrograph of $\text{SiO}_x/\text{Al}/\text{SiO}_x$ sandwich. Thickness of: SiO_x 10 to 20 nm, Al 30 to 50 nm, SiO_x 10 to 20 nm

Influence of the release layer on the bare aluminum reflectivity

The thickness and evaporation conditions of the NaCl release layer affect the optical reflectivity of the particles, even if the evaporation conditions are appropriate for Al alone.

At constant thickness of the release layer, the Al reflectivity is becoming light yellow when the pressure increases. A similar effect is observed at constant vacuum and increasing thickness of the release layer. Both observations are now fully understood but go beyond the scope of the present paper. All samples were then made with a 50 nm thick release layer of NaCl under a vacuum better than 10^{-4} mbar.

Effect of the SiO_x layer on the optical properties of $\text{SiO}_x/\text{Al}/\text{SiO}_x$ flakes SiO_x

Coated Al in air features a slightly lower reflectivity than the bare, unprotected Al, as shown in Figure 3, where each curve is the average of 5 different evaporation batches. The SiO_x coated Al batches were heated in air at 200°C for 1 hour in an attempt to fully oxidize the SiO_x layers.

The index of refraction of SiO_x , $x \sim 1.8$ is very close to the one of SiO_2 [11] and the loss in reflectivity cannot arise only from the difference in refraction index between SiO_x and air. More detailed investigations are required to understand this slight alteration of the reflectivity.

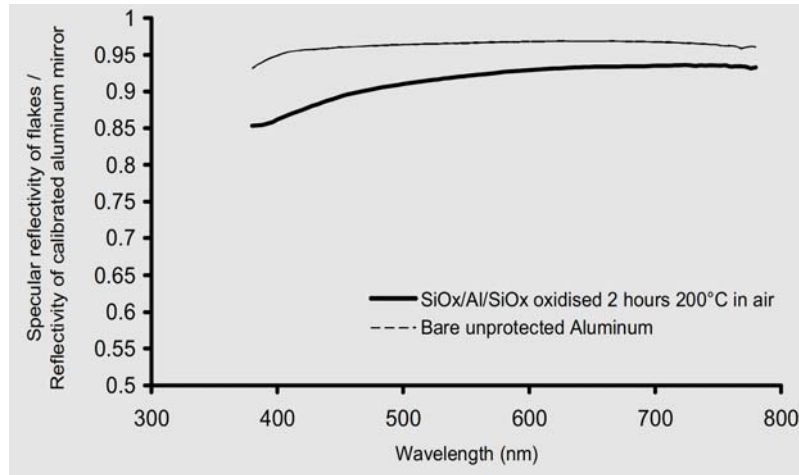


Figure 3. Reflectivity of bare aluminum flakes (--) and heated SiO_x protected Al flakes (—).

3.1.3. Water resistance of $\text{SiO}_x/\text{Al}/\text{SiO}_x$ flakes

Both protected and unprotected aluminum feature hydrogen generation in water set at pH of 8.0. The volume of hydrogen generated by protected aluminum flakes and unprotected ball milled aluminum is reported in Figure 4. The silica based protecting layer postponed the start of hydrogen generation by about 24 hours. The total amount of evolved hydrogen corresponds to the full conversion of metal Al in Al hydroxide. Optimizations are still required.

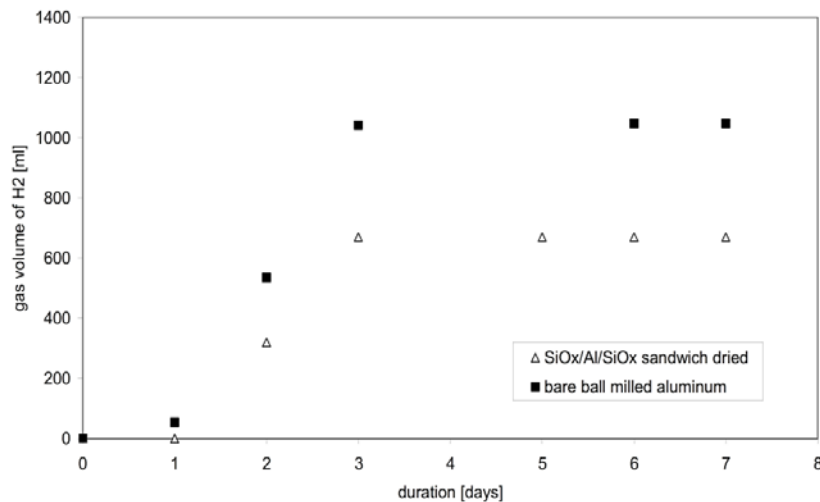


Figure 4. Amount of generated hydrogen in protected (Δ) an unprotected Al (\blacksquare) by aqueous Corrosion medium (2% Akropal N100). The gas volume is standardized on the Al content.

Porous SiO_x flakes

The co evaporation of the release layer and SiO_x allows making highly porous SiO_x flakes, as shown in Figure 5 [12].

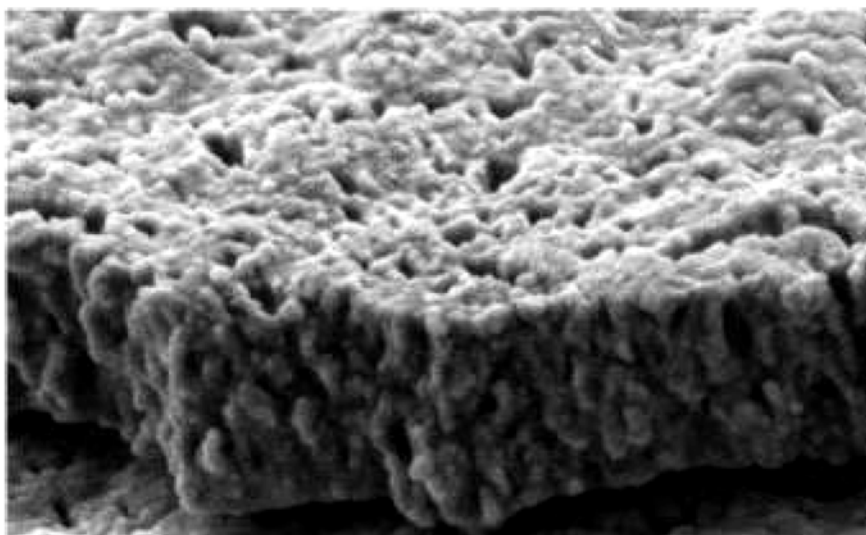


Figure 5. SEM micrograph of porous SiO_x flake. The estimated pore density is $3 \cdot 10^9 \text{ gcm}^{-2}$. The root mean square (RMS) roughness is between and 3 and 20 nm. Pore sizes according to BET measurements are between 2 and 5 nm with a maximum at 3 nm.

The porosity depends on the ratio NaCl/SiO_x and can be adjusted from 0 to close to 70%. The “pore” backbone consists of a percolating network of channels with a diameter of a couple of nanometers. The flake thickness is 50 nm or higher and its specific surface ranges from 500 to 900 m²/g. Such porous substrates can be loaded with metallic silver particles. The handling of large flakes with nano holes filled with silver is easier than that of powder of silver nano particles [13].

Conclusions

In the present study, SiO_x coating was applied by PVD method on aluminum alloys. Subsequently, its effect on raising the high-temperature oxidation resistance was analyzed.

The obtained results can be summarized as follows:

1. Conditions and features coatings had a major impact on the properties and performance of their coatings.
2. Reflective index properties of the coated samples are lower than uncoated samples.
3. The coating on samples reducing the rate of increase of hydrogen on the surface.
4. The deposition of coating on samples are often porous. The number, size and distribution of the pores are determined depending on the conditions of deposition.

References

- [1] A.S. Sanchez, I.P. Baena, J.A. Pomposo, Advances In Click Chemistry for Single-Chain Nanoparticle Construction, *Molecules* 2011, 13, 3279-3285.
- [2] E. Almeida, D. Santos, J. Uruchurtub, Corrosion Performance of Waterborne Coatings for Structural Light Alloy, *Progress in Organic Coatings, Volume 18, Issues 3-4, 2009, Pages 121-134*
- [3] A. Bailão, S. Šustic, Retouching With Mica Pigments, *E-Conservation Journal* 2, 2012, Pp. 35-44
- [4] R. Besol, W. Reisserand E. Roth, Oxidized Coloured Aluminum Pigments, *The Xeromorphic Engineer*, 07Nov. 2009, 258-265.
- [5] A. Gungora, H. Demirtasa, I. Atilgana, M. Yasarb, Synthesis and Characterization of SiO₂ Films Coated on Stainless Steel by Sol-Gel Method, *International Iron & Steel Symposium, Karabük, Türkiye, 02-04 April 2012, 213-219.*
- [6] W. Li, H. Tian, B. Hou, Corrosion Performance of Epoxy Coatings Modified by Nano Particulate SiO₂, *Materials and Corrosion, Volume 43, Issue 2, 2010, Pages 21-27.*
- [7] X. Shi, T.A. Nguyen, Z. Suo, Y. Liu, R. Avci, Effect of Nanoparticles on the Anticorrosion And Mechanical Properties of Epoxy Coating, *Surface & Coatings Technology* 132 (2008) 247-255
- [8] S. Wu, X. Li, Preparation of Pure Nano-Grained Si₂N₂O Ceramic, *International Journal of Refractory Metals and Hard Materials, Volume 13, 2008, Pages 97-103*
- [9] S. Wetzel, M. Klevenz, H. P. Gail, A. Pucci and M. Trieloff, Laboratory Measurement of Optical Constants of Solid SiO₂ and Application to Circumstellar Dust; *Astronomy & Astrophysics, A67(2013), 431-436.*
- [10] G.A. Breaux, R.C. Benirschke and M.F. Jarrold, Melting, Freezing, Sublimation, and Phase Coexistence in SiO₂ Nano Crystals, *Journal of Chemical Physics* Volume 125, Number 17 2008, 97-103.
- [11] K. Kranthi, A. Kurati, R. Dittmann, A. Vital, U. Klotz, P. Hug, T. Graule and M. Winterer, Silica-Based Composite And Mixed-Oxide Nanoparticles From Atmospheric Pressure Flame Synthesis, *Journal of Nanoparticle Research* (2009) 12: 320-326.
- [12] S. Mandal, B.D. Kulkarni, Separation Strategies for Processing of Dilute Liquid Streams, *International Journal of Chemical Engineering, Volume 2011, Article ID 659012, 19 Pages*
- [13] H. Hoppe, C. Bujard, Antimicrobial Porous Silicon Oxide Particles, United States Patent Application 20090214606.